Water-templated growth of interfacial superglue polymers for tunable thin films and *in-situ* fluid encapsulation

*Venkata S.R. Jampani[1,2], Miha Škarabot[2], Urban Mur[3], Damien Baigl[4], Ulrich Jonas[5], Jan P. F. Lagerwall[1], Miha Ravnik[3], Manos Anyfantakis[1]**

[1]Department of Physics and Materials Science, University of Luxembourg; L-1511, Luxembourg

[2]Condensed Matter Physics Department, Jožef Stefan Institute; 1000 Ljubljana, Slovenia

[3]Faculty of Mathematics and Physics, University of Ljubljana; 1000 Ljubljana, Slovenia

[4]PASTEUR, Department of Chemistry, École Normale Supérieure, PSL University, Sorbonne Université, CNRS, 75005 Paris, France.

[5]Department of Chemistry and Biology, University of Siegen; D-57076, Siegen, Germany

*Corresponding author. Email: anyfas.com@gmail.com

Keywords: superglue, interfacial polymerization, thin films, poly(cyanoacrylate), biodegradable polymers, fluid encapsulation

Thin polymer films are indispensable elements in numerous technologies ranging from liquid encapsulation to biotechnology to electronics. However, their production typically relies on wet chemistry involving organic solvents or chemical vapor deposition, necessitating elaborate equipment and often harsh conditions. Here, we demonstrate the eco-friendly, fast, and facile synthesis of water-templated interfacial polymers based on cyanoacrylates (superglues) that yield thin films with tailored properties. Specifically, by exposing a cationic surfactant-laden water surface to cyanoacrylate vapors, surfactant-modulated anionic polymerization produces a manipulable thin polymer film with a thickness growth rate of 8 nm/min. Furthermore, the shape and color of the film are precisely controlled by the polymerization kinetics, wetting conditions, and/or exposure to patterned light. Using various interfaces as templates for film growth, including the free surface of drops and soap bubbles, the developed method advantageously enables in-situ packaging of chemical and biological cargos in liquid phase as well as the encapsulation of gases within solidified bubbles. Simple, versatile, and biocompatible, this technology constitutes a potent platform for programmable coating and soft/smart encapsulation of fluids.

1. Introduction

Thin polymer films (TPFs) are layers of polymer materials with a uniform thickness from a few nanometers to micrometers. Due to their reduced dimensions, TPFs exhibit unique properties and serve as ideal platforms for exploring fundamental soft matter questions, e.g., the confinement effect on the dynamics of the constituent chains[1], or for developing technologies ranging from biological applications[2] to anticorrosion coatings[3], water-repellent fabrics[4], and wearable electronics[5]. This multitude of applications necessitates the development of methods delivering TPFs with well-controlled properties that are simple and cost-effective. Physical methods like spin-[6] and dip-coating[7] or layer-by-layer assembly[8] rely on dissolving a prefabricated polymer, which is then deposited on a substrate. Despite their capability to control film thickness, such methods rely on solvents, often expensive or harmful organic liquids requiring special handling. Chemical vapor deposition methods overcome this limitation by employing *in-situ* polymerization of reactants through the gas phase directly above the substrate[9]. Despite the excellent control of film properties, demanding conditions, typically low pressure and high temperature, are required. Besides the specialized equipment needed, this imposes constraints on the utilized materials and the process scaling up. Plasma-enhanced chemical vapor deposition uses reactive plasma species to activate monomers at lower temperatures, enabling TPF synthesis even at atmospheric pressure[10], as shown by polymerizing monomers inside sessile droplets on a substrate[11]. Despite the great potential of plasma deposition methods, the strong dependence of film quality on operating parameters and the need for noble gases limit their widespread use.

We envisaged that using cyanoacrylates (CAs), readily available monomers that rapidly polymerize under environmental conditions would be a practical strategy for preparing TPFs. CAs and their polymers (PCAs) are commercially important due to their suitability for plentiful applications[12]. Methyl- and ethyl cyanoacrylate (ECA) are industrially valuable because they are the basis of instant adhesives. Larger CAs like butyl and octyl CA are used to close wounds[13], partly due to their bacteriostatic properties[14]. CAs are also used in multiple fields, from fingerprint visualization in forensics[15] to multifunctional coatings[16]. The extended utility of CAs stems from their high reactivity. Weak nucleophiles like OH^- from water (*e.g.*, moisture on a surface) initiate rapid anionic polymerization, producing large macromolecules almost instantaneously[17]. The reactivity of CAs, however, makes their use for preparing nanomaterials with controlled morphology challenging[18]. Overcoming this limitation would allow for further CA exploitation for demanding applications beyond those already shown, *e.g.*,

fabricating superhydrophobic surfaces[19], recyclable plastics[20], and gel polymer electrolytes for flexible lithium batteries[21]. Besides, PCAs are also biocompatible[18,22] and biodegradable[14,23], which renders them excellent candidates for drug delivery, either as nanospheres[24] or nanocapsules[25]. Despite the widespread use of PCA in biomaterial applications[26] and the vast relevant research[27], fundamental chemistry aspects are still being explored[28]. Hence, if one wishes to unleash the potential of CAs for making precisely engineered materials suitable for emergent applications like liquid encapsulation[29,30] and flexible electronic paper in color[31], new synthesis methods that are well-controlled, versatile, and cost-effective are desired.

To address these challenges, we introduce a concept called WRAPPINGS (Water-based, Room temperature, Atmospheric Pressure Polymerization of Instant Glues controlled by Surfactants). It comprises a minimal system and an eco-friendly method to produce thin PCA films in a straightforward yet highly modular fashion. WRAPPINGS involves the exposure of a cationic surfactant-enriched air-water interface to CA vapor, which initiates anionic polymerization with chain growth confined to the interface and controlled by the surfactants. The resulting TPF has uniform thickness with less than 2% variation over 1 cm^2 area, which can be accurately tuned by adjusting the reaction time, thanks to a thickness growth rate of ~ 8 nm/min. We showcase the potential of this new technology for making and using TPFs on demand with three paradigms. First, by patterning the fluid interface shape and modulating the film thickness, we produce planar films of arbitrary size, shape, and tunable interference color. Second, by combining the polymerization scheme with aqueous templates of different forms, we demonstrate the *in-situ* packaging and manipulation of chemical cargos that is equally applicable to biological ones. Finally, we encapsulate and handle inert and reactive gases *in situ* by templating the polymerization with soap bubbles.

2. Results and Discussion

2.1. **PCA film formation at a surfactant-laden aqueous interface using WRAPPINGS.** Fig. 1 illustrates the WRAPPINGS concept for making thin PCA films using aqueous cationic surfactant (dodecyltrimethylammonium bromide, DTAB) solutions exposed to CA vapors coming from the air phase. We dispense a DTAB solution drop onto a substrate located in a Petri dish. Once a lid carrying ECA drops is placed on the dish, polymerization begins (t_{pol}= 0, Fig. 1*a*). The volatile monomer[27] quickly evaporates and creates an ECA-rich atmosphere. When ECA molecules reach the fluid interface, water molecules initiate anionic

polymerization. The hydroxide anion from self-dissociation of water attacks the β carbon of the double bond, yielding a carbanion, which grows further by subsequent monomer addition[32]. The rapid polymerization rate is due to the strong electron-withdrawing ester and cyano groups in the α-carbon, which stabilize the carbanion[33]. Movie S1 shows a highly reflective film appearing first at the center of the drop surface before propagating outwards to cover the entire surface. The film color, uniform across its whole surface due to the presence of surfactants (discussed later), is initially silver and progressively changes with t_{pol}, becoming gold at t_{pol} = 12 min (Fig. 1*a*, inset), purple, green, and then again purple. A greenish film is observed when the monomer supply is stopped by removing the lid at t_{pol}= 30 min. By removing the solution under the film (Movie S2), we obtain a dry, vividly green poly (ethyl cyanoacrylate) (PECA) film (*SI Appendix*, Fig. S1). The film displays varying colors with changing viewing angle. Commercial superglue was used in this experiment, but similar results were obtained with pure ECA (*SI Appendix*, Fig. 2).

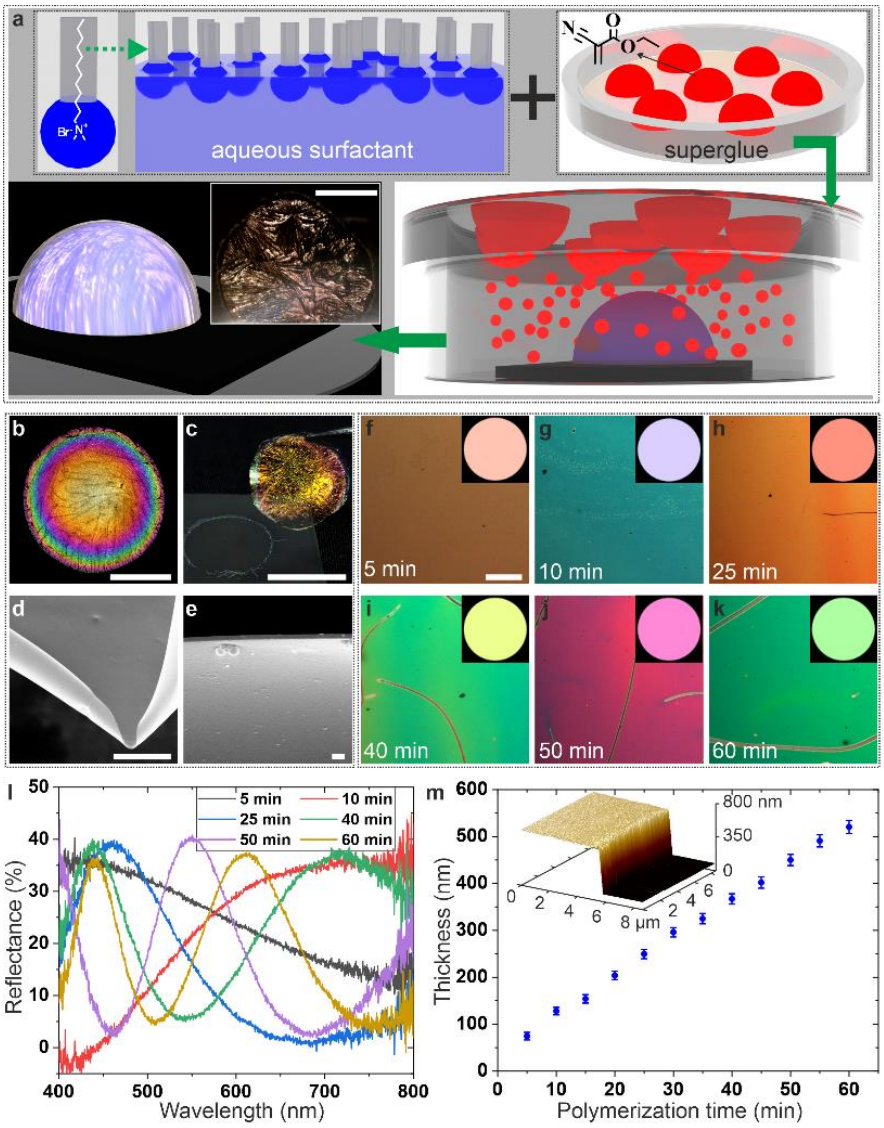

Figure. 1. Eco-friendly poly(cyanoacrylate) film synthesis at a surfactant-laden air-water interface using WRAPPINGS. (a) Schematic of the experimental system. The essential components are an air-water interface containing cationic surfactant molecules (DTAB, marked blue) and ECA liquid monomer (super glue, marked red) in the upper panel. This system is practically realized by enclosing a sessile drop of aqueous DTAB solution in a culture dish that is covered with a lid carrying superglue droplets (bottom right). ECA monomers in the vapor phase (red spheres) polymerize upon contact with the air-water interface, forming PECA chains that create a film over the sessile DTAB droplet (bottom left). Inset: reflection micrograph of a PECA film on DTAB solution (C_s= 2 mM) at t_{pol}= 12 min (Movie S1). (b) Reflection micrograph of a PBCA film. (c) Photograph of a free-standing PECA film held by forceps. Both films (b, c) were grown on DTAB solution (C_s= 3 mM, t_{pol}= 40 min) and deposited on the substrate after water removal. (d, e) SEM images of free-standing films grown on DTAB solutions. The top-view of a PECA film (C_s= 0.5 mM, t_{pol}= 120 min) shows a smooth surface (d), whereas the cross-section of a PBCA film (volume 3.5 mL, C_s= 0.5 mM, t_{pol}= 60 min) reveals its sub-µm thickness (e). (f-k) Reflection micrographs of PECA films grown onto DTAB solutions (C_s= 2 mM) for various t_{pol} and transferred onto Si wafers. Color results from thin-film interference are verified by simulations (insets), reflection microspectroscopy (l), and

thickness measurements using AFM (m). Scale bars are 1 cm (a, b, and c), 10 µm (d), 1 µm (e), and 100 µm (f-k).

The versatility of WRAPPINGS is evident in its compatibility with other cyanoacrylates like butyl (BCA) and isopropyl cyanoacrylate (Fig. 1*b*, *SI* Appendix, Fig. 3). Interestingly, PCA films can be made self-standing by detaching them from the substrate (Fig. 1*c*, Movie S3), which facilitates the investigation of their microscopic morphology. Scanning electron microscopy (SEM) images of PECA (Fig. 1*d*, *SI Appendix,* Fig. S4) and PBCA films (Fig. 1*e*, *SI Appendix,* Fig. S5) reveal a smooth topography. The softer PBCA (glass transition temperature $T_{g,\,PBCA}$ = 113 ºC[12]) film exhibits more folding than the more rigid PECA ($T_{g,\,PECA}$ = 132 ºC[12]) film. This permits the observation of its cross-section, revealing a uniform film thickness ($d_f \approx 308 \pm 19$ nm) along the portion (~70 µm wide) imaged (*SI Appendix*, Fig. S5).

To elucidate the influence of reaction time on their properties, we grow a series of PECA films on DTAB solutions by keeping C_s fixed and varying t_{pol} (*SI Appendix*, Fig. S6) that are then transferred onto Si wafers (Movie S4). Reflection microscopy shows that films grown for $t_{pol} \leq$ 30 min become almost wrinkle-free during the transfer process (*SI Appendix,* Fig. S7), unlike those produced for longer t_{pol} that maintain many wrinkles (*SI Appendix*, Fig. S8). The wrinkle density increases with t_{pol}, suggesting a Young's modulus increase with t_{pol}[34]. The film color is homogeneous over macroscopic (~cm^2) areas and changes with t_{pol} (Fig. 1*f-k*). Microspectroscopy reveals that the color results from broad reflection peaks (Fig. 1l, *SI Appendix*, Fig. S9). We hypothesize that longer t_{pol} results in thicker films, leading to variation in color and an increase in film elasticity. Atomic force microscopy (AFM) shows a linear d_f increase with t_{pol}, with a growth rate of ~8 nm/min. The thickness of the film was measured by imaging the edge of the film (Fig. 1*m* inset, *SI Appendix,* and Fig. S10). The surface roughness of films grown for different t_{pol} remains unchanged ($R_q \approx$ 4 nm, *SI Appendix,* Fig. S11), which agrees with the smooth surface observed with SEM. For these experiments, WRAPPINGS can achieve a d_f range spanning a decade (from ~75 nm to ~520 nm). The shape of the reflection spectra combined with d_f values on the order of visible light wavelengths suggests that the color-producing mechanism is thin-film interference. To verify this, we calculate the reflectance using the thin-film interference model for plane waves (*SI Appendix,* Figs. S12-S15). Colors obtained by transforming the calculated spectra into RGB images using the same color transfer functions as in the camera closely match with the experimental micrographs (Fig. 1*f-k*).

2.2. **Fundamental mechanism behind WRAPPINGS.** To gain insight into WRAPPINGS, we performed a series of control experiments. First, we replaced DTAB with the cationic surfactant hexadecyltrimethylammonium bromide (CTAB, *SI Appendix*, Fig. S16*a*). Both surfactants produce mechanically robust and colored films, underlining the importance of the amphiphilic nature of the surfactant for the film formation process. In particular, the positively charged head group of the surfactant, located at the air-water interface, creates a 2D template for the growth of the polymer chains. This allows efficient access to the supply of monomers from the gas phase, which directly reach the anionic active sites of the growing chains at the polymer-water interface (*SI Appendix*, Fig. S17), electrostatically attracted to the cationic head groups. Secondly, we challenged the need for cationic surfactants by growing PECA films on bare, ultrapure water. The result is significantly different, as the films are broken, transparent, colorless, and cannot be kept self-standing (*SI Appendix*, Fig. S18). The film fragility is due to the lower film thickness d_f (≈40 nm for t_{pol}= 20 min), suggesting a comparatively slow TPF growth on pure water (*SI Appendix*, Information). This indicates that the dissociation equilibrium between the positive surfactant head group and the active anionic ECA chain end supports larger ion separation and, consequently, fast polymerization rates. In the absence of cationic surfactants, the dissociation equilibrium involves protons more tightly associated with the active site, thus reducing the polymerization rate. Thirdly, using NaBr solutions as subphase yields colorless, fragile films similar to those grown on pure water (*SI Appendix*, Fig. S16*b*). These results rule out a strong influence of well-solvated Br^- anions (also present in the cationic surfactants) on the TPF growth rate. As a fourth control experiment, we investigate the role of electrostatic charge using the anionic surfactant sodium dodecyl sulfate (SDS) in the subphase. This yields colorless TPFs (*SI Appendix*, Fig. S19), contrary to the color observed with cationic surfactants. These experiments support our hypothesis that interfacial cations are vital to the rapid yet controlled PCA film growth. The quaternary ammonium head group of DTAB is bulky, resulting in a weaker association with the active PECA chain end. Additionally, water, a highly polar solvent, promotes ion dissociation. To further scrutinize this hypothesis, we introduce the polycation poly(L-lysine) into the aqueous subphase. This leads to colored TPFs of similar quality to those corresponding to cationic surfactants (*SI Appendix*, Fig. S20), confirming that cations near the aqueous interface significantly accelerate TPF growth. It is important to note that WRAPPINGS differs fundamentally from earlier works that demonstrated the stabilization of colloid monolayers at the air-water interface by poly

(cyanoacrylate) films[35], as well as the interfacial polymerization in heterogeneous systems (e.g., emulsions)[36,37], which neither targeted nor achieved control over the film properties.

WRAPPINGS bears a resemblance to differences in reaction pathways, based on different alkyl substitutions, observed when CAs react with substances such as tertiary amines, which are known to promote adhesion between surfaces[38,39] (*SI Appendix*, Information). Furthermore, our experiments reveal that colored TPFs form on solutions of triethylamine (*SI Appendix*, Fig. S21) or sodium bicarbonate (*SI Appendix*, Fig. S22), both known to yield high molecular weight PCAs[39,40]. Notably, a concentration of at least 1 mM is required for these substances to lead to qualitatively similar colored films, in stark contrast to the few μM needed with DTAB, illustrating a three-order magnitude higher concentration requirement. This significant difference arises because hydrophilic polycations, amines, and salts dissolve in the bulk aqueous phase, while surfactants accumulate at the surface. As a result, cationic surfactants ensure sufficient surface concentration at a much lower bulk concentration (*SI Appendix*, Information). The critical role of cationic surfactant is further emphasized by FTIR experiments indicating the presence of DTAB within the PECA films (*SI Appendix*, Fig. S23). We conjecture that the cationic heads form complexes with the growing polymer chains that make up the uniform TPF at the aqueous interface.

2.3. **Tunable planar films: programming shape, size, and color.** Using an air-water interface as a template for interfacial polymerization opens possibilities for manipulating the shape and geometry of TPFs. To illustrate this, we create a heart-shaped interface by confining a DTAB solution within a hydrophilic region patterned on a hydrophobic substrate using corona treatment. Upon exposure to ECA, a heart-shaped film with homogeneous azure color forms (Fig. 2*a*, *SI Appendix*, Fig. S24). This film patterning approach can be extended to curved substrates if the solution volume is kept low enough for capillary forces to hold it in place. One example of such a conformal film is shown in Fig. 2*b*; this silver PECA film in the shape of Luxembourg is formed on a ping-pong ball (*SI Appendix*, Fig. S24). The same approach is used in Fig. 2*c*–*d*, *SI Appendix*, Fig. S25 to make silvery films shaped like Z and O (t_{pol} =10 min), but for the latter, we modify the color to orange *after* the end of the initial polymerization by re-exposing the film to ECA. An additional polymerization step initiated by moisture adsorbed on the film increases d_f to alter the interference color. In another example, we dry an E-shaped DTAB solution drop, driving surfactant deposition onto the substrate area defined by the pattern. We then fabricate an E-shaped PECA film by adding water onto the substrate and exposing the resulting solution to ECA (Fig. 2*e*, *SI Appendix*, Fig. S25).

We can also manipulate the physical properties *within a single* PECA film by spatially modulating the polymerization kinetics. This is achieved by replacing DTAB with a photosensitive cationic surfactant, AzoTAB[41]. AzoTAB is an azobenzene trimethyl ammonium bromide surfactant that undergoes an isomerization from a *trans*-rich state to a more polar *cis*-rich state upon UV irradiation at 365 nm (*SI* Appendix, Fig. S26). This photo-induced polarity change results in UV-induced depletion of surfactant at the interface[42], increase in surface tension[43], and decrease in cooperative electrostatic interactions with oppositely charged objects, including colloids[44] and anionic polyelectrolytes[45]. Thus, we hypothesized that shining patterned UV light onto a drop exposed to ECA would enrich the non-irradiated area in cationic surfactants interacting more with ECA (here, trans-AzoTAB), and, therefore, locally accelerating the PECA growth. Fig. 2f-h shows films transferred onto Si wafers with a patterned Minoan double axe, the mythical Griffon, and the Eiffel tower (SI Appendix, Movies S5-S6 and Fig. S27). The color variation, from yellow for the irradiated area to turquoise for the dark area, confirms the greater df of the latter. These results confirm our proposed mechanism, where interfacial cations are instrumental in the TPF formation by modulating the chain growth. From a practical viewpoint, our approach enables us to prepare TPFs with programmable color patterns using an external stimulus that can be easily controlled in time and in space.

2.4. In-situ packaging of chemical and biological liquid cargos. WRAPPINGS further expands into encapsulating aqueous liquids, a topic that has received increased attention recently[29,30]. Here, we expose a pendant DTAB solution drop to ECA vapor, resulting in a PECA film on its surface. The accompanying decrease in air-drop interfacial tension results in a pear-like shape (Fig. 3a). After an adequate tpol to yield a mechanically robust polymer membrane, we stop the monomer supply and inject more liquid into the elastic liquid package. We then gently shake the partially encapsulated drop and place it on a substrate, ensuring that only the polymerized part touches it. Re-exposing the drop to ECA leads to polymerizing its bare part and a complete liquid enclosure with PECA. This results in a self-standing, dumpling-shaped encapsulated liquid package (Fig. 3b). This liquid package can be easily manipulated and transported with a pair of tweezers (Fig. 3c) or placed on different surfaces without sticking to them (SI Appendix, Movie S7 and Fig. S28). Compared to state-of-the-art methods for encasing macroscopic aqueous drops with polymer, WRAPPINGS eliminates the necessity of either organic solvents (of lower density than water) supporting a prefabricated TPF that encapsulates a drop falling on it[29], or a polymer dissolved in an organic solvent with specific properties (i.e., appropriate

water miscibility and interfacial tension)[30]. Furthermore, liquid dumplings are fully wrapped by a TPF with tunable thickness, as opposed to liquid marbles, which are drops partially covered by solid particles[46].

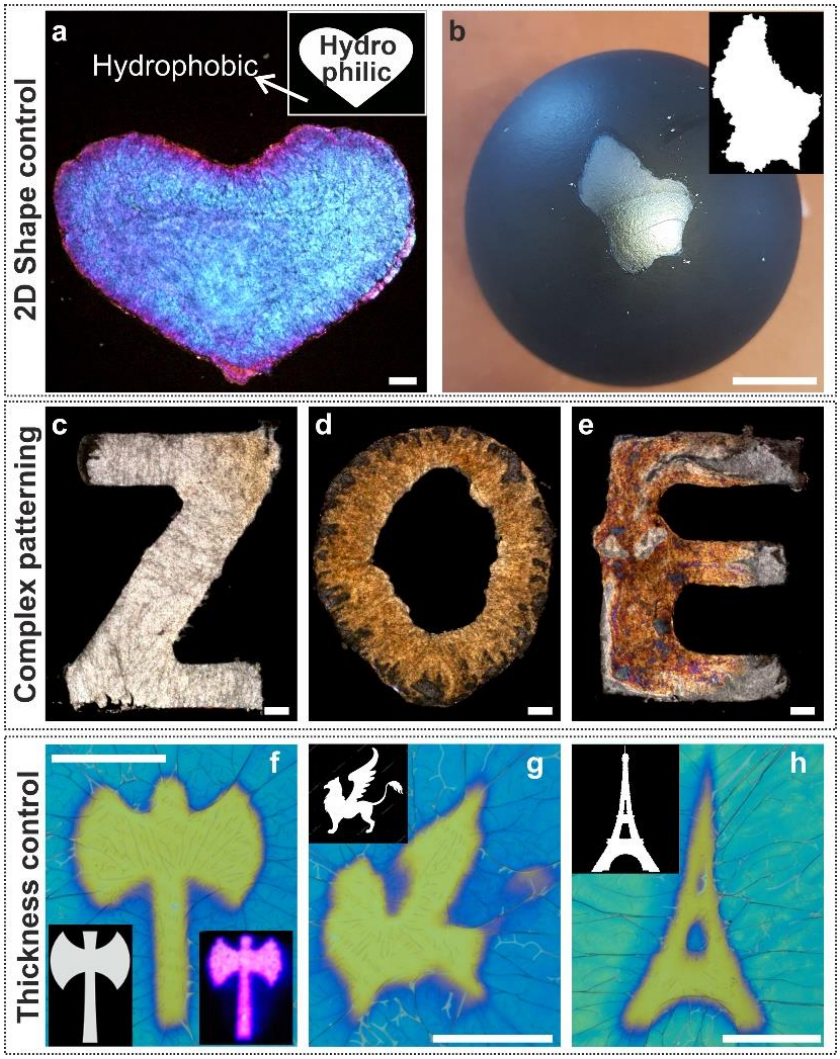

Figure. 2. Thin PECA films with tailored size, shape, and color. Exposure of shaped DTAB solutions (Cs= 2 mM, 40 µL), created with wettability patterns, to ECA vapor yields (a) a heart-shaped PECA film on a planar substrate (tpol = 20 min) or (b) a curved PECA film, with the shape of Luxembourg, conforming to the supporting ping-pong ball (tpol = 5 min). (c-e) Other strategies for preparing complex-shaped films (SI Appendix, Fig. S25). A Z-shaped DTAB solution (Cs = 2 mM, 20 µL) is exposed to ECA (tpol = 10 min), yielding a dry, silver-colored film (c). An O-shaped dry film is created the same way before being re-exposed to ECA vapor (tpol = 10 min), which leads to a color change from silver to orange (d). An E-shaped, multicolor film is created by water addition (22 µL) onto a pre-deposited DTAB pattern and exposure (tpol = 10 min) to ECA (e). (f-h) Two-color films are created by irradiating drops of photosurfactant (AzoTAB) solutions (Cs = 5 mM, 100 µL) with structured UV light (wavelength 365 nm), simultaneously exposed to ECA (tpol = 25 min). The films are transferred onto Si wafers after the polymerization ends. Examples of PECA films with patterns of the Minoan double axe (f), mythical Griffon (g), and Eiffel tower (h). Insets: the photomasks used

(f-h) and a UV pattern example (f). Scale bars are 1 mm (a), 1 cm (b), 100 µm (c-e), and 1 mm (f-h).

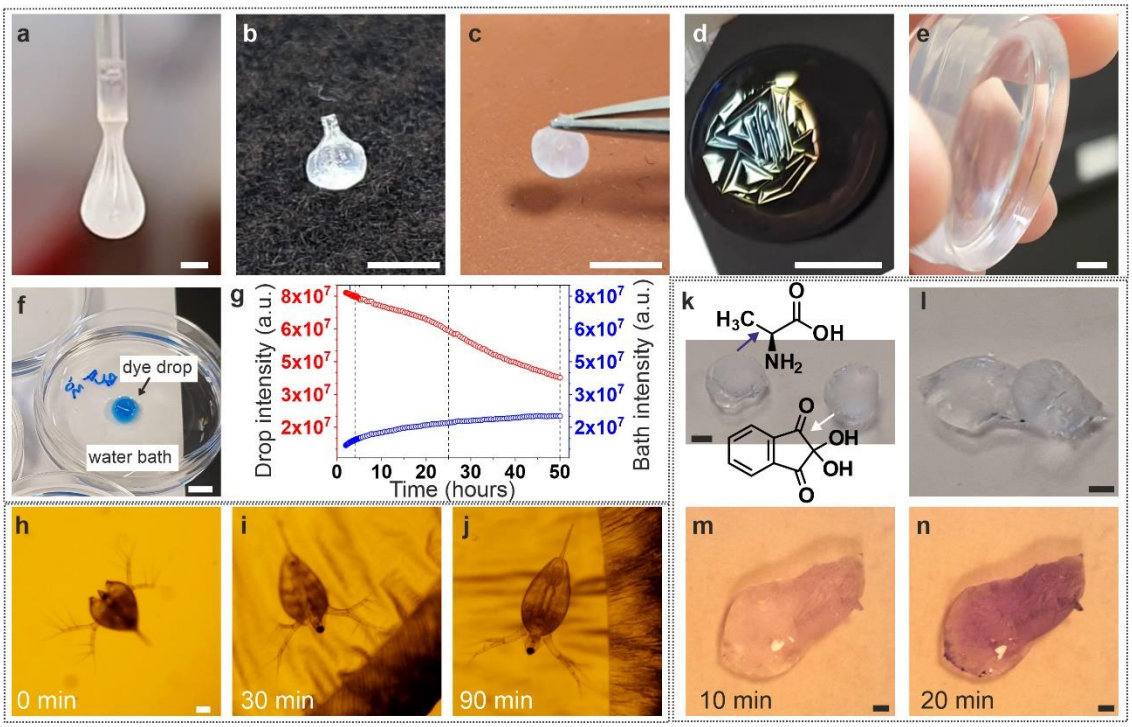

Figure. 3. Encapsulation of aqueous chemical and biological cargos. (a-c) The creation of free-standing liquid dumplings involves wrapping a DTAB solution pendant drop (Cs= 0.2 mM, ~10 µL) with PECA (a), followed by detaching the drop to completely polymerize it by re-exposing it to ECA (b). The liquid package can be manipulated with tweezers (c). (d-f) Growing PBCA of varying thickness on large DTAB solution volumes can (d) immobilize a 200 µL puddle (Cs= 50 µM, tpol= 10 min) on a tilted substrate, (e) contain ~7.5 mL of solution (Cs= 0.2 mM, tpol = 3 h) in a dish even placed upside-down, and (f) make a ~10 µL sessile drop (DTAB + methylene blue, tpol = 30 min) withstand partial immersion in water, while preventing dye leaching. Conversely, df. can be decreased (tpol = 2 min) to allow dye release from a drop (10 µL) of DTAB solution (Cs = 0.5 mM) and Rhodamine B into a phosphate-buffered saline solution. The release kinetics is followed in real-time by monitoring the fluorescent intensity of the drop and bath, respectively (g). (h-j) In-situ encapsulation of a drop (Cs= 100 µM, 200 µL) containing a Daphnia (h) with a biocompatible PBCA film. The swimming Daphnia is observed until the end of polymerization (tpol = 30 min) (i) and even 60 min later (j). (k-l) Following the method in (a-c), we form two PECA dumplings containing alanine and ninhydrin (both 1 wt.%) and DTAB (Cs= 0.2 mM, k). Real-time monitoring of the aminoacid-indicator reaction gradually turns the initially transparent liquid into purple upon squeezing the dumplings against each other (l). The time after mixing is indicated (m-n). Scale bars are 1 mm (a), 5 mm (b-f), 100 µm (h-j), and 1 mm (k-n).

WRAPPINGS may be further used to preserve (e.g., by slowing down drying) or protect (e.g., from contamination) aqueous samples by sealing them with a TPF. The softer polymer PBCA is used to encapsulate a large (~200 µL) puddle, preventing the liquid from flowing when

inclined (Fig. 3d, Movie S8). Significant liquid volumes (~7.5 mL) can also be encapsulated by increasing df, so liquid cannot flow out of the dish even upon reversal (Fig. 3e, SI Appendix, Movie S9). To further highlight the liquid packaging robustness, we wrap a sessile drop containing methylene blue with a PBCA film, which keeps the drop intact upon immersion in water while preventing dye diffusion (Fig. 3f). Conversely, the film permeability can be adjusted by changing df. We show this by encapsulating a drop containing Rhodamine B with a thinner PBCA film. Upon drop immersion in phosphate-buffered saline solution, the dye progressively diffuses into the buffer, with half released over ~50 h (Figs. 3g, SI Appendix, Fig. S29 and Movie S10). To our knowledge, these are the first demonstrations of the direct TPF syntheses onto aqueous specimens to encapsulate them. Recent works (e.g., on initiated CVD for enclosing low vapor pressure organic liquids with polymer[47] or plasma-induced polymerization at atmospheric pressure for encapsulating acrylate-based reactive liquids[48]), although limited to organic liquids, highlight the potential of liquid packaging.

Notably, in Fig. 3g-j, PBCA is synthesized utilizing a commercial product used for veterinarian surgery[49]. This is because PBCA has low toxicity and is biodegradable, making WRAPPINGS an ideal strategy for the non-invasive, in-situ encapsulation of living organisms[37]. To demonstrate this, we expose a drop containing a small planktonic crustacean, Daphnia, to BCA (SI Appendix, Information). Water contains DTAB at Cs= 100 μM that is low enough not to harm Daphnia, nonetheless adequate to accelerate TPF growth (Fig. 3h, SI Appendix, Movie S11). The transparent PBCA allows us to observe that the swimming behaviour of Daphnia remains unaltered during polymerization (Fig. 3i, Movie S12), and for over 60 min after the polymerization (Fig. 3j, Movie S13).

The capability of PCA films to confine aqueous liquids into self-standing objects (Fig. 3a-c) opens numerous possibilities for open microfluidic (i.e., channel-less) operations. This is demonstrated by creating two self-standing drops containing alanine and ninhydrin, respectively (Fig. 3k). Ninhydrin is an indicator used to detect amino acids like alanine, and their reaction produces a chromophore called Ruhemann's purple[50]. Bringing the two packages into contact results in their piercing and, in turn, liquid mixing (Fig. 3l), enabling the reaction that progressively turns the initially clear mixture to purple (Fig. 3m, n, SI Appendix, Movie S14). The optical clarity of the film allows observation by the unaided eye, thus following the reaction evolution in real time without any equipment. Our packaged liquids have attractive properties similar to liquid marbles[46] (e.g., non-sticking nature, transparency) without the constraint of utilizing nanoparticles with specific wettability[51] or size[52].

2.5. In-situ gas encapsulation and manipulation with solid bubbles. We next show that WRAPPINGS can also be used to encapsulate and manipulate gaseous samples in situ. Previous studies have shown that gas encapsulation is achievable in the microscale (~1-20 μm) by the layer-by-layer assembly of polyelectrolytes onto microemulsion bubbles[53]. Our conceptually different strategy utilizes soap bubbles, thin films of water, and glycerol stabilized by surfactants (Fig. 4a). In the first example, we create a spherical bubble by injecting air into a tip containing soap bubble solution. We then detach the bubble by gently shaking it and placing it on a fabric (Fig. 4b). The resulting quasi-spherical bubble is polymerized by passing ECA vapor through the fabric, yielding a PECA film on its outer surface (Figs. 4c, SI Appendix, Fig. S30 and Movie S15). We can destabilize the bubble by piercing it with a sharp object (Fig. 4d, SI Appendix, Movie S16), which results in a collapsed, elastic TPF with vivid colors (Fig. 4e). Although quasi-spherical, polymerized bubbles can remain stable for several months (SI Appendix, Fig. S31), it is challenging to maintain a freshly created bubble during an adequate polymerization time leading to a robust TPF. To tackle this challenge, we use a partially wetting substrate to generate a hemispherical bubble that shows superior stability against popping (Fig. 4f). Upon ECA exposure, the outer surface of the bubble is polymerized, creating a dome-shaped elastic film (SI Appendix, Fig. S32). This geometry allows dispensing ninhydrin and alanine solution drops (Movie S17), thanks to the self-healing nature of soap films[54]. Subsequent polymerization with ECA vapors transforms the bubble into a solid reactor (Movie S18). Its transparency allows for visual monitoring of the occurring reaction, as evidenced by the drop turning purple (Fig. 4h, SI Appendix, Fig. S33). The reaction product can also be collected by cutting the chamber with a scalpel (Fig. 4i, SI Appendix, Movie S19).

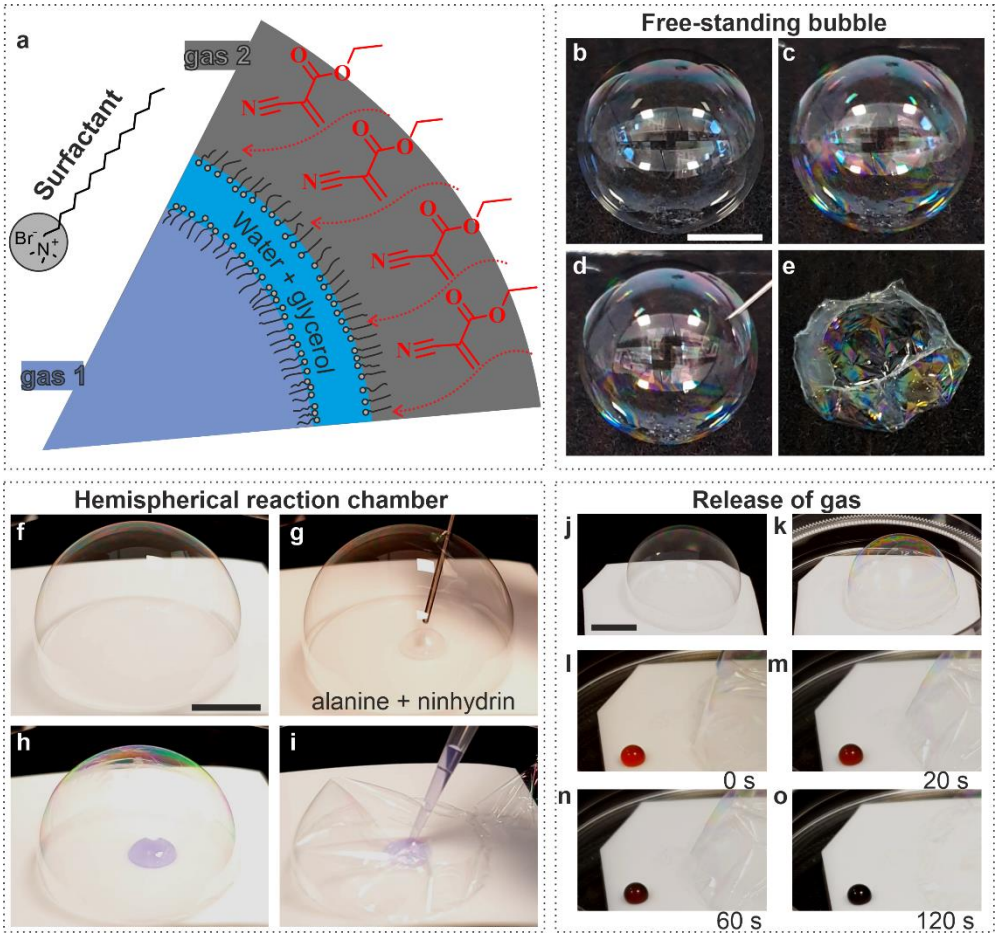

Figure. 4. Encapsulating and handling gaseous specimens. (a) Schematic of a soap bubble comprising a film of hexadecyltrimethylammonium bromide (CTAB) and glycerol solution that is solidified by ECA introduced in the outer gas (a). (b-e) A quasi-spherical air bubble (~5 mL) enclosed by ~10 µL of CTAB (Cs= 6 mM) and glycerol (20 wt. %) aqueous solution is created (b) and polymerized by ECA vapor diffusing through the supporting cloth for tpol= 10 min (c). Piercing with a needle results in a colorful, elastic film collapsing onto the fabric (d, e). (f-i) We form a PECA reaction chamber by first making a hemispherical bubble (6 mL) with an aqueous solution of CTAB (Cs= 5.95 mM) and glycerol (30 wt. %) on a PTFE substrate (f), in which we dispense two drops containing alanine (1.05 wt. %) and ninhydrin (1.04 wt. %) using a needle prewetted with bubble solution (g). The transparent PECA chamber (tpol= 10.5 min) allows the (h) real-time monitoring of the aminoacid-indicator reaction progress via the color change in the drop and (i) collecting the reaction product. (j-o) After making a sessile bubble containing 8 mL of air saturated with acetic acid using a solution of CTAB (Cs= 5.94 mM) and glycerol (20.1 wt. %) on a PTFE substrate placed in a dish (j), we polymerize it for tpol= 10 min (k). We then dispense a drop containing Congo Red (0.04 wt. %) next to it. At t = 0, the gas is released by breaking the bubble (l), whereafter, it gradually diffuses into the drop to lower its pH, leading to a progressive color change from red to black (m-o). All scale bars are 1 cm.

Solid bubbles can also incorporate reactive gases that participate in a chemical reaction. To show this, we form a solid bubble that contains acetic acid mixed with air (Fig. 4j-k, Movie

S20) next to a solution drop of Congo Red, a pH-sensitive dye. The drop remains red, indicating that the enclosed gas is contained within the bubble (Movie S21). The gas-dye reaction is initiated by breaking the bubble (Fig. 4l), which allows the acidic gas to diffuse away. This causes the drop to gradually turn dark red and eventually black (Fig. 4m-o). Other gases, such as inert CO2 or more reactive gases like triethylamine, can also be enclosed (SI Appendix, Fig. S34).

3. Conclusion

WRAPPINGS is a novel concept yielding biocompatible TPFs with customizable microscopic and macroscopic properties that relies on the polymerization of superglues on aqueous interfaces containing interfacial cationic species (*e.g.*, surfactants, polyelectrolytes). The simplicity of this concept is demonstrated by the capability to prepare thin PCA films even at home, using materials used in everyday life, without requiring specialized equipment (*SI Appendix,* Fig. S35 and MovieS22). This results in a modular platform with unique outcomes, including complex TPFs with spatially or temporally controlled thickness and interference color (*SI Appendix,* Fig. S36). Additionally, WRAPPINGS allows *in-situ* encapsulation of various aqueous and gaseous specimens, including living organisms and reactive and inert chemicals. The ability to customize the PCA chemistry[55] and thickness potentially allows for the programmable release of drugs, liquids, and gases into physiological or other environments[56], as well as the stabilization of fluid interfaces for robust heterogeneous systems[36] and self-standing liquids without using specifically engineered nanoparticles[46]. These aspects make WRAPPINGS a powerful yet eco-friendly platform for several demanding operations. Fundamentally, the action of cationic species as stabilizing accelerators enables the exploration of analogous effects in other systems. We hope our study will act as a seed for further innovation by scientists and engineers across multiple disciplines.

4. Experimental Methods

The WRAPPINGS concept involves the exposure of the surface of an aqueous solution containing cationic species that act as stabilizing accelerators for the polymerization of cyanoacrylate monomer. Hence, there are three key ingredients: water, a cationic substance, and a monomer. We tested how various substances, both laboratory-grade and commercial products used in everyday life, perform as core ingredients for WRAPPINGS. For more information on those, as well as all other materials used for the film synthesis and encapsulation

experiments (e.g., salts, dyes, Daphnia, gases), and the experimental setup (e.g., substrates, sample cells, polymerization chambers), see the Supplementary Information.

TPF generation. In a typical experiment, as illustrated schematically in Fig. 1, an aqueous surfactant solution is placed inside a chamber in which polymerization occurs. The solution may be either in the form of a sessile drop or a larger liquid puddle deposited on a solid substrate, a large liquid volume held within a black plastic lid, a pendant drop, or a quasi-spherical or sessile bubble resting on a substrate. The reaction chamber may be either a culture dish or a jar (see Supplementary Information). In any case, the desired number of monomer drops is dispensed on the top (or bottom) surface of the reaction chamber. A positive displacement pipette (Multipette M4, Eppendorf, Germany) is used to i) make monomer drops of precise volume (typically 4 µL each) and ii) ensure that the pipette is not contaminated by polymer forming on any surface containing water moisture. The reaction chamber is closed with a lid immediately after the monomer drops are placed on it; this is the onset of the polymerization (t_{pol}= 0). We assume the polymerization starts rapidly; this is based on the high volatility of the cyanoacrylates used: the boiling points of ECA, ICA, and BCA are 54 ºC (at 0.21 kPa), 53 ºC (at 0.27 kPa), and 83 ºC (at 0.40 kPa), respectively[27]. Experiments generating planar TPFs are performed in an incubator with a controlled temperature (25 ºC); the ambient relative humidity is typically in the ~38-64 % range.

Isolation of TPFs from the air-water interface. Thin PECA films formed on the free surface of drops may be deposited onto the supporting solid substrate by removing all water (and almost all surfactant) under the film. This is achieved by combining the usage of paper tissue, enabling most of the solution to be drained via capillary forces and evaporation that removes the remaining water (Movie S2). Dry deposited films may be lifted from the substrate (Movie S3) and transferred to another substrate. Alternatively, TPFs formed either on the surface of water puddles (including photopatterned films) or on larger volumes of water contained within lids may be transferred onto solid substrates using another procedure involving floating the films on a large volume of ultrapure water. This enables the complete removal of surfactants while reducing film wrinkling (Movies S4-S5).

Generation of planar TPFs of arbitrary shape and size. To create a planar or curved film of arbitrary shape and size, we shape the free interface of the surfactant solution by placing it on a substrate having a wettability pattern. We start with a flat or curved substrate, first coated with

a material based on silicone resin (see Supplementary Information), which renders the substrate black and hydrophobic. Next, we place the desired pattern on a paper sticker (SI Appendix, Fig. S24 a, e) on the hydrophobic substrate. A corona plasma treater (Corona SB, BlackHole Lab) is used to make the unprotected surface of the substrate hydrophilic. After removing the sticker, a wettability pattern is created comprising a hydrophilic area surrounded by a hydrophobic one. Dispensing the appropriate volume of surfactant solution on the hydrophilic part leads to a free interface of the desired size and shape (*SI Appendix,* Fig. S24 b). Cyanoacrylate polymerization on this shaped interface is conducted as described above, leading to shaped TPFs (*SI Appendix,* Fig. S24 c-d, f-i).

Generation of liquid dumplings. Apart from planar interfaces, any aqueous entity, regardless of its shape, may be used as a template for growing PCA films. To demonstrate the potential of WRAPPINGS for packaging liquids, we first form a pendant DTAB solution drop (volume on the order of ~ 10 µL) using a 1 mL plastic syringe (Injekt® F, Braun) and a PTFE needle with 1 mm diameter (KRÜSS GmbH, Germany). The pendant drop is then exposed to ECA vapor, which leads to a thin PECA film covering its surface. Once a sufficient t_{pol} has passed to yield a mechanically robust polymer membrane, we stop the monomer supply. We then inject more liquid into the elastic micro-balloon to increase its weight. By gently shaking the needle, we detach the partially encapsulated drop and place it on a solid substrate, ensuring that only the polymerized part of the drop encounters the substrate. We subsequently expose the drop once again to ECA vapor to polymerize the bare part of it and, hence, fully enclose the liquid with PECA. All liquid dumpling experiments were conducted in ambient temperature (~22-24 ^{o}C) and relative humidity (~38-64 %) conditions.

Generation and solidification of soap bubbles. A soap bubble, a thin liquid film stabilized by a bilayer of surfactants, constitutes an ideal platform for handling gases while including the key components required to form a TPF using WRAPPINGS. From a practical perspective, to polymerize a soap bubble using our concept, it is imperative to prepare long-lasting bubbles, i.e., with a lifetime of at least several minutes. Although various recipes for making long-lasting soap bubbles are available, they typically rely on commercial dishwashing liquids (see ref. [57] and references therein). Apart from containing numerous substances at unknown concentrations, commercial formulations contain mostly anionic surfactants; this is incompatible with WRAPPINGS, necessitating the use of cationic species. For these reasons, we developed our own aqueous solutions (which we call bubble solutions) able to yield bubbles that remain stable

long enough for WRAPPINGS to be efficient in solidifying them (*i.e.*, on the order of ~ 5 min). Our bubble solutions were prepared by adding in a vial, in this order, the appropriate amount of ultrapure water, concentrated aqueous CTAB solution, and glycerol; different formulations were tested, and the exact concentrations of each substance are given in the figure corresponding to each experiment reported here. Typically, these samples were mixed gently by hand (to avoid forming bubbles) and then heated to ~50 ^{o}C for a few minutes to achieve homogenization. The homogeneous bubble solutions were kept in an orbital mixer for an additional ~ 2h.

We explored two different bubble geometries. First, we form a spherical soap bubble using either a 10 or a 20 mL plastic syringe (Injekt®, Braun) with an attached rubber tube connected to a plastic micropipette tip (Eppendorf). Air is injected into the micropipette tip that contains a small volume (typically on the order of ~10 µL) of the bubble solution. By gently shaking the tip, we detach the bubble and deposit it as a quasi-spherical, self-standing object on a fabric. Next, we pass ECA vapor through the porous fabric, and the quasi-spherical bubble solidifies as a PECA film forms on its outer surface. Second, using the same setup and procedure described above, we initially create a small spherical bubble, which we bring in contact with a partially wetting substrate. Upon touching the solid surface, it becomes a sessile bubble with a dome shape. The size of the sessile bubble can be adjusted by injecting additional air into it. Sessile bubbles are polymerized following the procedure used for sessile drops of surfactant solutions. All bubble polymerization experiments were conducted in ambient temperature (~22-24 ^{o}C) and relative humidity (~38-64 %) conditions.

Photopatterning setup for making PECA films with two-color patterns. A home-built optical setup irradiated sessile drops of aqueous AzoTAB solution that were exposed to ECA vapors (*SI Appendix*, Fig. S26). UV light (wavelength 365 nm) from an LED source (CoolLED pE-300 White) was delivered to an inverted fluorescence microscope (Ti2-U Eclipse, Nikon) by means of a liquid light guide (CoolLED). Photomasks were prepared by printing the desired pattern twice on transparent plastic foils with a printer. The photomasks were cut in the size and shape of optical filters and were inserted in the light path. The resulting light pattern was focused on the free surface of the sessile drop using a microscope objective (10x, Nikon). The drop was dispensed on a poly(styrene) substrate (culture dish lid, diameter 38 mm), itself placed in a culture dish (diameter 100 mm, volume≈ 173 cm^2); the latter was covered with a lid, onto which 8 drops (4 µL each) of ECA (commercial superglue) were dispensed. All photopatterning

experiments were conducted in a temperature range of ~22-23 ^{o}C and a relative humidity range of ~38-64 %.

Modeling of thin film interference colors. We used the principles of thin film interference to calculate the refractive index of the film and model the colors of reflected light[58]. Our model consists of 3 layers: an air layer with a refractive index, $n_a = 1$, a thin film of unknown refractive index, n_f and thickness, d_f, and a SiO_2 substrate, n_{SiO2} (*SI Appendix,* Fig. S12). The SiO_2 substrate used has a thickness of 650 microns and is considered infinite in the model. We considered the refractive index of SiO_2 as constant with the value of $n_{SiO2} = 1.465$ [59] and assumed a normal incidence angle.

To determine the refractive index of the film, we analyze the experimental reflectance spectra of films and corresponding thicknesses, d_f, measured using AFM. Initially, we identify the positions of transmittance minima and maxima in the spectra, which indicate constructive or destructive interference and are linked to the phase shifts of the reflected waves. For the assumption $n_a < n_f > n_{SiO2}$ we obtain the constructive

$$2n_f d_f = m\lambda, m = 0.5,1.5,2.5, \ldots \quad \textbf{(Eq. 1)}$$

and destructive interference

$$2n_f d_f = m\lambda, m = 0,1,2, \ldots \quad \textbf{(Eq. 2)}$$

conditions, respectively. We analyze the range of wavelengths between 410 nm and 720 nm to identify the peaks correctly. To achieve this, we filter out the measurement noise and smoothen the spectra curves using the moving average of 85 data points. Using this method, we identify the peaks of 39 different reflectance spectra of films with nine different thicknesses (*SI Appendix,* Fig. S13, a). We then create a plot that displays the wavelength at which each of the extrema (minima or maxima) occurs against the film thickness (*SI Appendix,* Fig. S13, b). By applying Eq. 1 and Eq. 2, extrema with the same values of $m$are positioned along the line with the same slope, which we use to determine m for each extremum.

After *m* for each extremum is identified, we can use the relation: $\frac{m\lambda}{2} = n_f d_f$, following Eq. 1 and Eq. 2, to determine the refractive index of the film from the slope of the plot. The result is shown in *SI Appendix,* Fig. S14. The calculated value of the refractive index of the film is $n_f = 1.505 \pm 0.022$, and the R-squared value of the fit is above 0.98. Note that we did not take into account the possible error in the thickness measurement during the calculation.

Once the refractive index of the film is known, we can calculate the reflectivity of the system using the Fresnel equations. The reflection coefficient of light passing through a boundary between two layers with different refractive indices is calculated as

$$r = \frac{n_1 - n_2}{n_1 + n_2} \qquad \textbf{(Eq. 3)}$$

while the transmission coefficient is calculated as

$$t = \frac{2n_1}{n_1 + n_2} \qquad \textbf{(Eq. 4)}$$

where the light propagates from a medium with n_1 into a medium with n_2 (3).
The spectral intensity of light S_{ref} reflected from our system, which consists of 3 layers, is calculated as

$$S_{\text{ref}}(\lambda) = \left(A^2 + B^2 + 2AB\cos(\phi_B(\lambda) - \phi_A)\right)S_{\text{in}}(\lambda) = C_{ref}(\lambda)S_{\text{in}}(\lambda), \qquad \textbf{(Eq. 5)}$$

where the spectral intensity of the incoming light (*i.e.*, illumination) $S_{\text{in}}(\lambda)$, which is measured in the experiment, is multiplied by the coefficient $S_{\text{in}}(\lambda)$ that takes into account the interference between first and second-order reflections as described in the following and shown in *SI Appendix,* Fig. S12. The interference coefficient $C_{\text{ref}}(\lambda)$ is calculated from the sum of the two reflected waves, where $A = \left|\frac{n_a - n_f}{n_a + n_f}\right|$ is the ratio between the amplitude of the incoming light and the light that is reflected from the first boundary (between air and the film) and $B = \frac{2n_a}{n_a + n_f}\frac{n_f - n_{SiO2}}{n_f + n_{SiO2}}\frac{2n_f}{n_a + n_f}$ is the ratio between the amplitude of the incoming light and the light that is transmitted through the first boundary (between air and the film), reflected from the second boundary (between film and SiO_2), and transmitted through the first boundary again. $\phi_A = \pi$ is

the phase that is acquired by the first wave when reflected from the first boundary and equals to π, as $n_f > n_a$.

$\phi_B = 4\pi n_f d_f \lambda$ is the phase that is acquired by the wave with the amplitude B when passing through the film with the thickness d_f, being reflected from the second boundary and passing through the film again. No additional phase is acquired during reflection from the second boundary, as $n_{SiO2} < n_f$. Higher-order reflections and material refractive index dispersion are both neglected. The spectral intensity, which depends on the refractive index and the thickness of the film, is calculated by Eq. 3 and then transformed into an RGB picture using the same color functions and white balance values as in the Pixelink capture OEM software, used to generate experimental pictures. The resultant TPF color spectrum is shown in *SI Appendix*, Fig. S15.

Acknowledgements

We are indebted to Jacopo Vialetto for early-stage film characterization experiments and Athina Anastasaki, Richard Whitfield, and Nghia Truong Phuoc for experiments and fruitful discussions on poly(cyanoacrylate) characterization. We thank Martin Dulle for X-ray scattering experiments and Monique Wiesinger for technical support and several inspiring suggestions. We also thank Rijeesh Kizhakidathazhath, Maria Vamvakaki, Eleni Pavlopoulou, Emmanuel Stiakakis, Roberto Quintana, Mohan Srinivasarao, Syuji Fujii, Daniel Schmidt, and Damjana Drobne for fruitful exchanges at various stages of this research, and Igor Muševič and Albert Schenning for critically reviewing the manuscript. VSRJ is grateful to Igor Muševič and Matjaž Humar for allowing access to their laboratories and acknowledges valuable discussions with Polona Umek.

References

[1] B. Li, S. Zhang, J. S. Andre, Z. Chen, *Prog. Polym. Sci.* **2021**, *120*, 101431.

[2] A. Khlyustova, Y. Cheng, R. Yang, *J. Mater. Chem. B* **2020**, *8*, 6588.

[3] I. Vilaró, J. L. Yagüe, S. Borrós, *ACS Appl. Mater. Interfaces* **2017**, *9*, 1057.

[4] D. Soto, A. Ugur, T. A. Farnham, K. K. Gleason, K. K. Varanasi, *Adv. Funct. Mater.* **2018**, *28*, 1.

[5] T. L. Andrew, L. Zhang, N. Cheng, M. Baima, J. J. Kim, L. Allison, S. Hoxie, *Acc. Chem. Res.* **2018**, *51*, 850.

[6] D. B. Hall, P. Underhill, J. M. Torkelson, *Polym. Eng. Sci.* **1998**, *38*, 2039.

[7] E. Bindini, G. Naudin, M. Faustini, D. Grosso, C. Boissière, *J. Phys. Chem. C* **2017**, *121*, 14572.

[8] J. J. Richardson, M. Björnmalm, F. Caruso, *Science* **2015**, *348*, aaa2491.

[9] K. K. Gleason, *Nat. Rev. Phys.* **2020**, *2*, 347.

[10] D. Merche, N. Vandencasteele, F. Reniers, *Thin Solid Films* **2012**, *520*, 4219.

[11] U. Czuba, R. Quintana, M. C. De Pauw-Gillet, M. Bourguignon, M. Moreno-Couranjou, M. Alexandre, C. Detrembleur, P. Choquet, *Adv. Healthc. Mater.* **2018**, *7*, 1.

[12] Y. Barkan, M. Levinman, I. Veprinsky-zuzuliya, T. Tsach, E. Merqioul, G. Blum, A. J. Domb, A. Basu, *Acta Biomater.* **2017**, *48*, 390.

[13] A. J. Singer, J. V. Quinn, J. E. Hollander, *Am. J. Emerg. Med.* **2008**, *26*, 490.

[14] I. S. Bayer, *5 - Nanostructured Cyanoacrylates: Biomedical Applications*, Elsevier Inc., **2018**.

[15] S. P. Wargacki, L. A. Lewis, M. D. Dadmun, *J. Forensic Sci.* **2007**, *52*, 1057.

[16] M. T. Masood, M. Zahid, L. Goldoni, L. Ceseracciu, A. Athanassiou, I. S. Bayer, *ACS Appl. Mater. Interfaces* **2018**, *10*, 34573.

[17] H. W. Coover, D. W. Dreifus, J. T. O'Connor, *Handbook of Adhesives*, Van Nostrand Reinhold, New York, **1990**.

[18] E. Mele, J. A. Heredia-Guerrero, I. S. Bayer, G. Ciofani, G. G. Genchi, L. Ceseracciu, A. Davis, E. L. Papadopoulou, M. J. Barthel, L. Marini, R. Ruffilli, A. Athanassiou, *Sci. Rep.* **2015**, *5*, 1.

[19] L. Zhang, N. Zhao, X. Li, Y. Long, X. Zhang, J. Xu, *Soft Matter* **2011**, *7*, 4050.

[20] A. J. Christy, S. T. Phillips, *Sci. Adv.* **2023**, *9*, eadg2295.

[21] Y. Cui, J. Chai, H. Du, Y. Duan, G. Xie, Z. Liu, G. Cui, *ACS Appl. Mater. Interfaces* **2017**, *9*, 8737.

[22] J. M. Korde, B. Kandasubramanian, *Biomater. Sci.* **2018**, *6*, 1691.

[23] C. Vauthier, *Polymer Nanoparticles for Nanomedicines*, Springer International Publishing, Cham, **2016**.

[24] P. Couvreur, B. Kante, M. Roland, P. Guiot, P. BAuduin, P. Speiser, *J. Pharm. Pharmacol.* **1979**, *31*, 331.

[25] N. Al Khouri Fallouh, L. Roblot-Treupel, H. Fessi, J. P. Devissaguet, F. Puisieux, *Int. J. Pharm.* **1986**, *28*, 125.

[26] C. Vauthier, C. Dubernet, E. Fattal, H. Pinto-Alphandary, P. Couvreur, *Adv. Drug*

Deliv. Rev. **2003**, *55*, 519.

[27] P. Klemarczyk, in *Adhes. Sci. Eng.*, Elsevier, **2002**, pp. 847–867.

[28] R. Sáez, C. McArdle, F. Salhi, J. Marquet, R. M. Sebastián, *Chem. Sci.* **2019**, *10*, 3295.

[29] D. Kumar, J. D. Paulsen, T. P. Russell, N. Menon, *Science* **2018**, *359*, 775.

[30] S. Coppola, G. Nasti, V. Vespini, L. Mecozzi, R. Castaldo, G. Gentile, M. Ventre, P. A. Netti, P. Ferraro, *Sci. Adv.* **2019**, *5*, DOI 10.1126/sciadv.aat5189.

[31] K. Xiong, G. Emilsson, A. Maziz, X. Yang, L. Shao, E. W. H. Jager, A. B. Dahlin, *Adv. Mater.* **2016**, *28*, 9956.

[32] D. C. Pepper, *Makromol. Chemie. Macromol. Symp.* **1992**, *60*, 267.

[33] X. Zhang, X. Tang, K. Bowen, *Chem. Phys. Lett.* **2013**, *582*, 21.

[34] J. Huang, M. Juszkiewicz, W. H. de Jeu, E. Cerda, T. Emrick, N. Menon, T. P. Russell, *Science* **2007**, *317*, 650.

[35] N. Vogel, L. De Viguerie, U. Jonas, C. K. Weiss, K. Landfester, *Adv. Funct. Mater.* **2011**, *21*, 3064.

[36] X. Lian, S. Liao, X. Q. Xu, S. Zhang, Y. Wang, *Macromolecules* **2021**, *54*, 10279.

[37] J. Nicolas, P. Couvreur, *Nanomedicine and Nanobiotechnology* **2009**, *1*, 111.

[38] Y. Okamoto, P. T. Klemarczyk, *J. Adhes.* **1993**, *40*, 81.

[39] P. Klemarczyk, *Polymer (Guildf).* **2001**, *42*, 2837.

[40] D. H. Park, S. B. Kim, K. D. Ahn, E. Y. Kim, Y. J. Kim, D. K. Han, *J. Appl. Polym. Sci.* **2003**, *89*, 3272.

[41] A. Diguet, R.-M. Guillermic, N. Magome, A. Saint-Jalmes, Y. Chen, K. Yoshikawa, D. Baigl, *Angew. Chemie Int. Ed.* **2009**, *48*, 9281.

[42] J. Vialetto, M. Anyfantakis, S. Rudiuk, M. Morel, D. Baigl, *Angew. Chemie Int. Ed.* **2019**, ange. 201904093.

[43] N. Kavokine, M. Anyfantakis, M. Morel, S. Rudiuk, T. Bickel, D. Baigl, *Angew. Chemie - Int. Ed.* **2016**, *55*, 11183.

[44] M. Anyfantakis, D. Baigl, *Angew. Chemie Int. Ed.* **2014**, *53*, 14077.

[45] A. Estévez-Torres, C. Crozatier, A. Diguet, T. Hara, H. Saito, K. Yoshikawa, D. Baigl, *Proc. Natl. Acad. Sci.* **2009**, *106*, 12219.

[46] P. Aussillous, D. Quéré, *Nature* **2001**, *411*, 924.

[47] M. M. De Luna, P. Karandikar, M. Gupta, *Mol. Syst. Des. Eng.* **2020**, *5*, 15.

[48] F. Rezaei, M. D. Dickey, P. J. Hauser, *J. Appl. Polym. Sci.* **2020**, *137*, 6.

[49] F. Ollivier, M. Delverdier, A. Regnier, *Vet. Ophthalmol.* **2001**, *4*, 261.

[50] D. J. McCaldin, *Chem. Rev.* **1960**, *60*, 39.

[51] D. Zang, Z. Chen, Y. Zhang, K. Lin, X. Geng, B. P. Binks, *Soft Matter* **2013**, *9*, 5067.

[52] M. Anyfantakis, V. S. R. Jampani, R. Kizhakidathazhath, B. P. Binks, J. P. F. Lagerwall, *Angew. Chemie* **2020**, *132*, 19422.

[53] D. G. Shchukin, K. Köhler, H. Möhwald, G. B. Sukhorukov, *Angew. Chemie - Int. Ed.* **2005**, *44*, 3310.

[54] L. Courbin, H. A. Stone, *Phys. Fluids* **2006**, *18*, 10.

[55] C. Gross-Heitfeld, J. Linders, R. Appel, F. Selbach, C. Mayer, *J. Phys. Chem. B* **2014**, *118*, 4932.

[56] Z. Sheng, H. Wang, Y. Tang, M. Wang, L. Huang, L. Min, H. Meng, S. Chen, L. Jiang, X. Hou, *Sci. Adv.* **2018**, *4*, eaao6724.

[57] S. Frazier, X. Jiang, J. C. Burton, *Phys. Rev. Fluids* **2020**, *5*, 1.

[58] O. Stenzel, *The Physics of Thin Film Optical Spectra*, Springer International Publishing, Cham, **2016**.

[59] S. Chongsawangvirod, E. A. Irene, A. Kalnitsky, S. P. Tay, J. P. Ellul, *Proc. - Electrochem. Soc.* **1990**, *90*, 320.